

Associated network family of the unified piecewise linear chaotic family and their relevance

Haoying Niu(牛浩瀛) and Jie Liu(刘杰)

Citation: Chin. Phys. B, 2025, 34 (**4**): 040503. DOI: 10.1088/1674-1056/adb26a
Journal homepage: http://cpb.iphy.ac.cn; http://iopscience.iop.org/cpb

What follows is a list of articles you may be interested in

Fractional-order heterogeneous memristive Rulkov neuronal network and its medical image watermarking application

Dawei Ding(丁大为), Yan Niu(牛炎), Hongwei Zhang(张红伟), Zongli Yang(杨宗立), Jin Wang(王金), Wei Wang(王威), and Mouyuan Wang(王谋媛)
Chin. Phys. B, 2024, 33 (**5**): 050503. DOI: 10.1088/1674-1056/ad322b

A novel variable-order fractional chaotic map and its dynamics

Zhouqing Tang(唐周青), Shaobo He(贺少波), Huihai Wang(王会海), Kehui Sun(孙克辉), Zhao Yao(姚昭), and Xianming Wu(吴先明)
Chin. Phys. B, 2024, 33 (**3**): 030503. DOI: 10.1088/1674-1056/ad1a93

Transition to chaos in lid-driven square cavity flow

Tao Wang(王涛) and Tiegang Liu(刘铁钢)
Chin. Phys. B, 2021, 30 (**12**): 120508. DOI: 10.1088/1674-1056/ac3226

Application of the nonlinear time series prediction method of genetic algorithm for forecasting surface wind of point station in the South China Sea with scatterometer observations

Jian Zhong(钟剑), Gang Dong(董钢), Yimei Sun(孙一妹), Zhaoyang Zhang(张钊扬), Yuqin Wu(吴玉琴)
Chin. Phys. B, 2016, 25 (**11**): 110502. DOI: 10.1088/1674-1056/25/11/110502

Adaptive step-size modified fractional least mean square algorithm for chaotic time series prediction

Bilal Shoaib, Ijaz Mansoor Qureshi, Shafqatullah, Ihsanulhaq
Chin. Phys. B, 2014, 23 (**5**): 050503. DOI: 10.1088/1674-1056/23/5/050503

Associated network family of the unified piecewise linear chaotic family and their relevance

Haoying Niu(牛浩瀛)[1] and Jie Liu(刘杰)[1,2,†]

[1] *Research Center of Nonlinear Science, Wuhan Textile University, Wuhan* 430073, *China*
[2] *School of Mathematics and Physics Science, Wuhan Textile University, Wuhan* 430073, *China*

(Received 9 December 2024; revised manuscript received 23 January 2025; accepted manuscript online 5 February 2025)

Duality analysis of time series and complex networks has been a frontier topic during the last several decades. According to some recent approaches in this direction, the intrinsic dynamics of typical nonlinear systems can be better characterized by considering the related nonlinear time series from the perspective of networks science. In this paper, the associated network family of the unified piecewise-linear (PWL) chaotic family, which can bridge the gap of the PWL chaotic Lorenz system and the PWL chaotic Chen system, was firstly constructed and analyzed. We constructed the associated network family via the original and the modified frequency-degree mapping strategy, as well as the classical visibility graph and horizontal visibility graph strategy, after removing the transient states. Typical related network characteristics, including the network fractal dimension, of the associated network family, are computed with changes of single key parameter α. These characteristic vectors of the network are also compared with the largest Lyapunov exponent (LLE) vector of the related original dynamical system. It can be found that, some network characteristics are highly correlated with LLE vector of the original nonlinear system, i.e., there is an internal consistency between the largest Lyapunov exponents, some typical associated network characteristics, and the related network fractal dimension index. Numerical results show that the modified frequency-degree mapping strategy can demonstrate highest correlation, which means it can behave better to capture the intrinsic characteristics of the unified PWL chaotic family.

Keywords: nonlinear time series, unified PWL chaotic family, Lyapunov exponents, complex network

PACS: 05.40.–a, 05.45.–a, 05.45.Ac, 05.45.Gg, 05.45.Tp

DOI: 10.1088/1674-1056/adb26a **CSTR:** 32038.14.CPB.adb26a

1. Introduction

In the past two decades, the analysis of nonlinear dynamics through the modeling of complex systems from the perspective of network science has become one of the most important areas in physics, mathematics, and other interdisciplinary fields.[1,2] These methods have received wide attention from researchers all over the world. Almost all real objects can be described by network science tools via proper modelling methods. Complex networks are gradually becoming one of the best paradigms for describing different complex systems. Traditional nonlinear time series analysis methods are mainly based on classical statistical analysis; phase space reconstruction; recurrence analysis of time series; calculation of Lyapunov exponent, correlation dimension, fractal dimension, Kolmogorov entropy, etc.[3–5] Based on classical methods of statistical analysis have been relatively complete, to carry out phase space reconstruction is relatively cumbersome. Therefore, it is necessary to explore alternative methods for characterizing nonlinear time series.

Approaches to modeling and analysis from a network science perspective have proven to be useful in revealing the inner laws hidden in many complex systems. For example, Zhang *et al.* converted pseudo-periodic time series into complex networks and found that time series with different dynamics exhibit different topological structures, which indicates that complex network analysis can be used as an effective tool for dynamic analysis of nonlinear time series.[6] Subsequently, the analysis of nonlinear time series based on complex network theory has attracted wide attention.[2,7,8]

Particularly, Lacasa *et al*. proposed the natural visibility algorithm,[9] which efficiently and simply maps each data point in the time series to a node in the network, and the connecting edges depend on the visibility between the data points (if visible for each other, connecting edges will be added between these two nodes). They found that the associated network will inherit the dynamics of the original time series. Luque *et al*., proposed the horizontal visibility algorithm, which constructs the network based on the principle of horizontal visibility, simplifies the network structure and reduces the time complexity, and constructs the network with smaller average degree compared with the natural visibility algorithm.[10] Meanwhile, Marwan *et al*. proposed the recurrence network analysis method, which is to consider the points in phase space as nodes in the network and use the distance between the points in phase space to define the connection between the nodes, and if the distance is greater than a threshold

†Corresponding author. E-mail: liujie@wtu.edu.cn

© 2025 Chinese Physical Society and IOP Publishing Ltd. All rights, including for text and data mining, AI training, and similar technologies, are reserved.

then there exists a connecting edge between two nodes of the mapped network.[11] Campanharo *et al*. proposed an approximate inverse operant quantile graph method to transform a time series into a network and demonstrated that the network analysis method can be used to distinguish different dynamic states in time series.[12] In 2012, Zhou *et al*. introduced the limited penetrable distance based on the natural visibility algorithm and proposed the limited penetrable visibility graph, which inherits the simplicity of the natural visibility graph, has lower computational complexity, stronger anti-noise capabilities and can process long time series in real time.[13] Lacasa, *et al*., also extended visibility graph mapping algorithm to multivariate time series.[14] At the same period, Li *et al*. proposed the frequency-degree mapping algorithm by encoding the time series into the edges of a network to maintain the original characteristics of the time series; they used it in the classification of physiological data, such as ECG, and distinguished ventricular fibrillation (VF) and monomorphic ventricular tachycardia (MVT) from normal sinus rhythm (NSR) by extracting the average degree and average path length features of the constructed network, showing the potential application value of this type of algorithm.[17] Sun *et al*. proposed symbolic representations of the transformed network, in which they defined each symbol as a node in the network. The connectivity between nodes was characterized by different transfer probabilities between symbols.[18] Gao *et al*. constructed a network based on Markov transfer probabilities and constructed a directed weighted complex network with different time series, which could be used for state classification of multi-phase flow.[19] In recent several years, Walker *et al*. proposed the compression network algorithm, where the largest connected component of the resulting compression network can be used to distinguish between random and chaotic dynamics.[20] Liu *et al*. proposed a new modified quantile graph constructing method. This approach is based on the Markov transition probability, employing an equal-distance interval division strategy and this algorithm can distinguish different nonlinear time series effectively.[21] Wang *et al*. proposed a method for constructing multi-scale transition networks from time series based on phase space coarse-grained partitioning. Through the analysis of time series from both discrete and continuous systems, they found that the multi-scale entropy measures of the resulting networks have the same ability as Lyapunov exponents to successfully identify chaotic.[22] Wang *et al*. introduced the Sliding Window Limited Penetration Visibility Graph (SLPVG) method, which takes into account the dynamic characteristics of time series and the impact of noise. With relatively low computational complexity, it accurately captures the dynamic features and, combined with network topology metrics, effectively reflects circuit fault states.[23] For more advances on these hot directions, one can consult some newly published reviews, i.e. Refs. [15,16], etc. These advances show the potential power of network modelling analysis techniques from different aspects in almost all fields of scientific research.

In this paper, we will try to explore nonlinear dynamics of typical chaotic system under the viewpoint of network analysis methods according to some typical methods proposed in aforementioned literatures. It is quite different from the classical statistical analysis on nonlinear time series, i.e., phase space reconstruction method, etc. This paper will carry out investigations on the unified PWL chaotic system family, based on two typical network modeling and analyzing methods. We will investigate the associated network family of the unified PWL chaotic family via some effective transformation methods, which can reflecting the intrinsic nonlinear characteristics. We will try to find out whether there are some potential relationships between those two sets through the calculation and comparison of related network characteristics with the largest Lyapunov exponent of original nonlinear time series.

The article is organized as follows, Section 2 will give some preliminary concepts related to our paper, including the classical nonlinear feature of the unified PWL chaotic system family. Section 3 gives two typical algorithms for constructing associated networks under the viewpoint of complex networks. Section 4 will give two associated networks families of the unified PWL chaotic system family and calculate the network characteristics. Section 5 will conduct a relevance analysis between the largest Lyapunov exponent generated by the unified PWL chaotic system family and its corresponding network characteristics. Finally, the paper is summarized in Section 6.

2. The unified PWL chaotic family and its basic characters

2.1. The model of the unified PWL chaotic family

In 2004, Lü *et al*. proposed the generalized Lorenz-like system, a continuous chaotic system.[24] Subsequently, Liu *et al*. introduced a simple piecewise linear (PWL) system known as the unified PWL chaotic system.[25] This system is capable of bridging the gap between the PWL Lorenz system and the PWL Chen system, representing the entire family of chaotic systems that lie between them. For more dynamics analysis on this nonlinear system, one can consult the literature,[25] in which the authors conducted dynamics analysis of this new PWL system with a single key parameter. The equations describing the PWL chaotic family are listed as follows:

$$\begin{cases} \dot{x} = a(y-x), \\ \dot{y} = \operatorname{sgn}(x)(c-a\alpha-z) + (8\alpha-1)qy, \\ \dot{z} = \operatorname{sgn}(y)x - bz, \end{cases} \tag{1}$$

where $\operatorname{sgn}(\cdot)$ denotes the standard signum function, providing the sign of its argument. The constants a, c, b, q, and α

are parameters in the system equation. Here we set $a = 1.20$, $c = 7.0$, $b = 0.15$, $q = 0.10$. According to Ref. [25], for all parameter $\alpha \in [0.00, 1.00]$ this family of systems is chaotic.

For these fixed parameters values, there are some typical chaotic attractors, i.e., when $a = 1.20$, $c = 7.0$, $b = 0.15$, $q = 0.10$, and $\alpha = 0.000$, the dynamics belong to the PWL Lorenz chaotic system;[26] when $a = 1.20$, $c = 7.0$, $b = 0.15$, $q = 0.10$, and $\alpha = 0.125$, the dynamics belong to the PWL critical chaotic system;[27] when $a = 1.20$, $c = 7.0$, $b = 0.15$, $q = 0.10$, and $\alpha = 1.000$, the dynamics belong to the PWL Chen system.[28] Those attractors behaved different in structures. For more details, one can consult the related literature.[25] The corresponding two-dimensional (2D) and three-dimensional (3D) phase diagrams for the key parameter $\alpha = 0$ is plotted in Fig. 1. Additionally, the corresponding time series components of the trajectory are illustrated in Fig. 2. The key parameter $\alpha = 0.125$ is plotted in Fig. 3. Additionally, the corresponding time series components of the trajectory are illustrated in Fig. 4. The key parameter $\alpha = 1.00$ is plotted in Fig. 5. Additionally, the corresponding time series components of the trajectory are illustrated in Fig. 6.

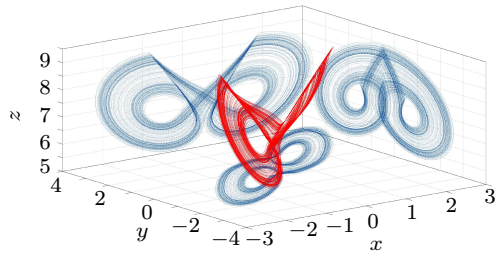


Fig. 1. The 3D (red online) attractor and 2D (blue online) portraits for the unified PWL chaotic family proposed when $\alpha = 0$.

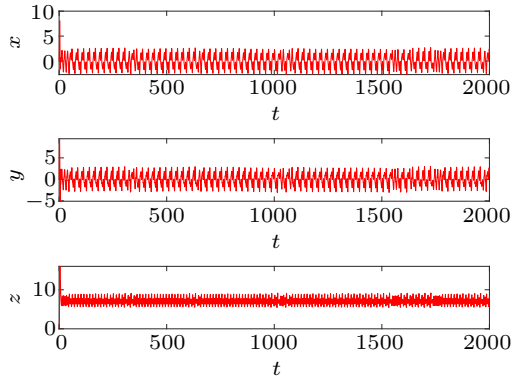


Fig. 2. Trajectory of the unified PWL chaotic family when $\alpha = 0$.

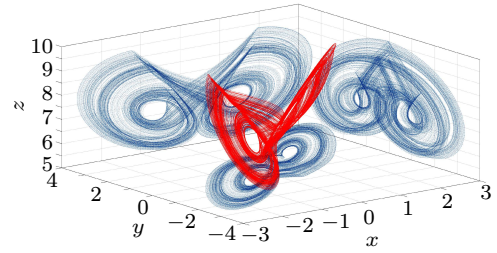


Fig. 3. The 3D (red online) attractor and 2D (blue online) portraits for the unified PWL chaotic family proposed when $\alpha = 0.125$.

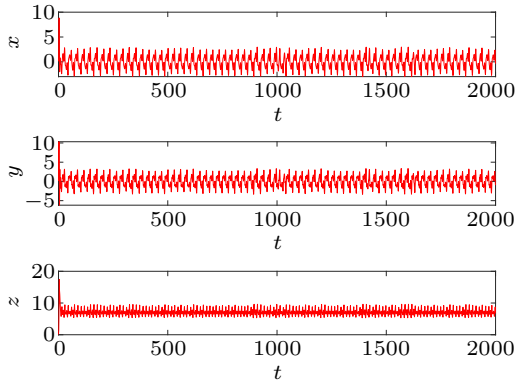


Fig. 4. Trajectory of the unified PWL chaotic family when $\alpha = 0.125$.

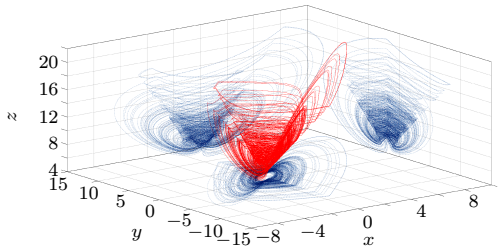


Fig. 5. The 3D (red online) attractor and 2D (blue online) portraits for the unified PWL chaotic family proposed when $\alpha = 1$.

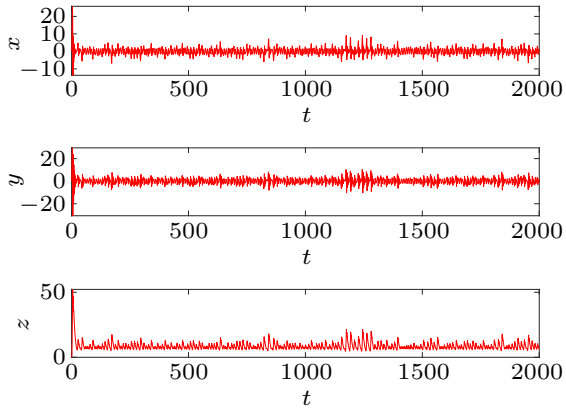


Fig. 6. Trajectory of the unified PWL chaotic family when $\alpha = 1$.

Remark 1 The unified PWL chaotic family with single parameter is something like the famous generalized Lorenz family (unified chaotic family).[24] These two famliy are typical cases of continuous chaotic systems and piecewise linear chaotic systems with single key parameter. For the PWL chaotic systems mentioned here, it can be physical fulfilled in circuits with lower price and both have potential usages in secret communication system designing.[29]

2.2. Lyapunov exponent of the unified PWL chaotic family

The Lyapunov exponent, first proposed by Lyapunov in 1907, provides a qualitative and quantitative characterization of the dynamical behavior of a system. Lyapunov exponent characterizes the rate of separation or attraction between neighboring trajectories within an attractor.[3] If a dynamical system has a positive Lyapunov exponent, this means that small perturbations of the initial conditions in this direction increase rapidly with time, corresponding to the local instability

of the orbit, and the system exhibits chaotic behavior. A negative Lyapunov exponent means that the system is convergent in this direction, and neighboring points eventually converge and merge into a single point, which corresponds to a stable point and periodic motion. A zero Lyapunov exponent indicates that the system is stable in this direction and the perturbations do not diverge or converge. A system with at least one positive Lyapunov exponent is defined as chaotic. The largest Lyapunov exponent, as the name suggests, is the largest of all Lyapunov exponents, and is a quantitative indicator to recognize that a dynamical system is chaotic. By utilizing the Wolf algorithm,[3,30,31] We compute the Lyapunov exponent. Randomly selecting initial values within [0, 1] × [0, 1] × [0, 1], we calculate the Lyapunov exponents of the unified PWL chaotic system family as the parameter α varies. The related results are shown in Fig. 7.

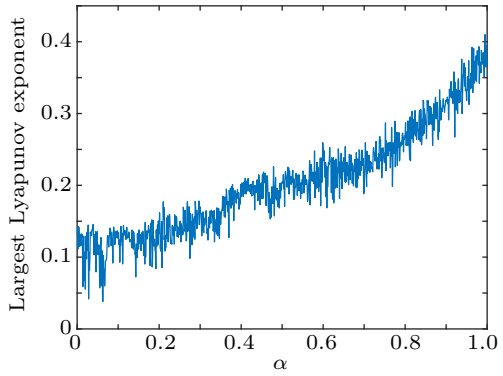


Fig. 7. The largest Lyapunov exponent spectrum of the unified PWL chaotic system family with respect to α.

From Fig. 7 we can find that for $0 < \alpha < 1$, the largest Lyapunov exponents of the system are all larger than zero, which hints the related dynamical system behaves as a chaotic state.

3. Associated networks constructed method via frequency degree mapping strategy

3.1. The original frequency degree mapping algorithm (FDM)

Order and reproduction situation are two key attributes in time series analysis. In order to deeply mine the characteristics of the original time series and transform the time series into a network, Li *et al*. proposed the frequency-degree mapping algorithm.[17] In this algorithm, each data point of the time series is mapped as a node of the network, and edges of the network are defined in two ways. The first is by temporal edges defined in chronological order. Specifically, temporal edges imply that each node is connected to its nearest left and right neighbors in chronological order, i.e., each node has two temporal edges. The second way is the recurrence edge obtained from the recurrent case of the original time series.

The original time series is processed by means of amplitude quantization, where all values distributed within the same quantization interval are assigned the same integer and are considered as recurrence. The more values distributed within the same quantization interval, the higher the reproduction frequency will be obtained. In this algorithm, there is a parameter K that represents the number of intervals divided.

Finally, the temporal edges and the recurrence edges are connected to form a new network. In simple terms, the frequency-degree algorithm connects each node to its nearest left and right neighbors in temporal order, and then the nodes located within the same interval are fully connected.

For illustration purposes, the univariate parameter in this algorithm is the quantization level K. The equation $I = H/K$ always holds during the amplitude quantization process, where H is the amplitude range of the original time series, and I is the quantization interval.

Step 1 Amplitude division: Through the quantitative analysis of the amplitude distribution, the reproduction frequency of the time series data is obtained; the equation $I = H/K$ always holds during the amplitude quantification process, where H is the amplitude range of the original time series, i.e., the difference between the maximum value and the minimum value of the time series, and the parameter K is the number of the intervals to be divided into K equal parts of the amplitude range H, and I is the length of each interval K from small to large corresponds to the interval from the minimum point to the maximum point of the time series, for the value on the boundary of the interval belongs to the larger intervals, the largest value in the time series belongs to the K_{th} interval.

Step 2 Time domain coding: Mapping the given time series to network nodes, i.e., each data point of the time series corresponds to a node of the network.

Step 3 Connected edge operation: Connecting nodes according to the time order and time series data reproduction frequency, i.e., each node is connected to its right and left neighboring nodes in the time order and the nodes in the same interval are fully connected.[17]

We give two schematics of the frequency-degree mapping algorithm for the illustrations in Figs. 8 and 9.

As shown in Fig. 8, we transform the time series 0.57, 0.22, 0.76, 0.36, 0.7, 0.95, 0.12, 0.82, 0.25, and 0.82 corresponding to the length of 10 into an associated network by using the frequency-degree algorithm N to take 4. The data values distributed in the same quantization interval are considered as reproducing nodes, and these reproducing nodes are connected to each other. For example, node 2, node 7, and node 9 form a cluster in the network, each node has two reproduction edges in addition to two temporal edges, the degree value of each node depends on the frequency of its reproduction, which is the reason why the method is called frequency-

degree mapping algorithm.

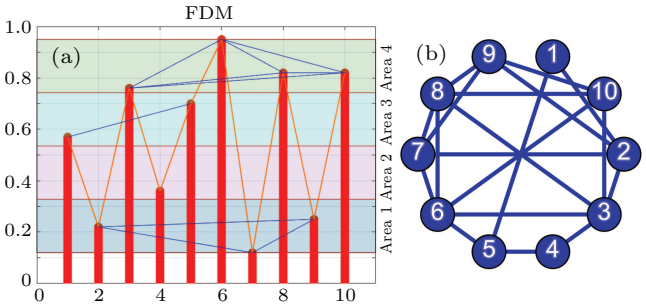


Fig. 8. Panel (a) is sample time series ([0.57, 0.22, 0.76, 0.36, 0.7, 0.95, 0.12, 0.82, 0.25, 0.82]) and panel (b) is its associated network derived from the frequency-degree mapping algorithm.

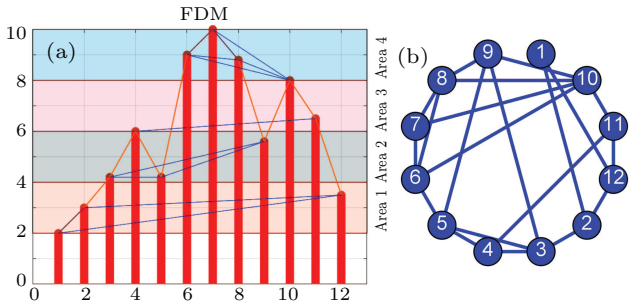


Fig. 9. Panel (a) is sample time series ([2, 3, 4.2, 6, 4.2, 9, 10, 8.8, 5.6, 8, 6.5, 3.5]) and panel (b) is its associated network derived from the original frequency-degree mapping algorithm.

As shown in Fig. 9, we transform the time series 2, 3, 4.2, 6, 4.2, 9, 10, 8.8, 5.6, 8, 6.5, 3.5, which corresponds to a length of 12, into a associated network using the original frequency-degree mapping algorithm, with K set to 4. Values located at the endpoints of the intervals are mapped to larger intervals, e.g., the fourth point of the time series corresponds to a value of 6 which is exactly at the endpoints of the intervals, and thus belongs to the area 3. The 7-th point in the time series corresponds to the time point with the largest value and belongs to the last interval, which is area 4.

The idea behind the original frequency-degree algorithm is that data with a high reproduction frequency will correspond to nodes with large degree values. In other words, the reproduced nodes will be fully connected to form a cluster in the associated network.

3.2. The modified frequency degree mapping algorithm (MFDM)

The modification is reflected in the different methods used to divide the intervals, unlike the traditional frequency-degree mapping algorithm which directly divides the amplitude intervals into equal parts, we further consider the positional information of the data points of the time series. Specifically, we remember that the length of the time series is N, and K is the parameter to be input, and if N is divisible by K, then these data points of the time series are divided into K intervals equally, and if N is not divisible by K, then these data points of the time series are divided into $K+1$ interval.

We consider the following two cases.

The case where N divides by K: If N divides by K, then the data points will be divided equally into these intervals, denoted as $d = N/K$, the time series will be sorted from the smallest to the largest, and the data points of the time series will be partitioned according to $[d : d : N]$, and the data points in the same interval will be connected to its two nearest neighbors on the left and right sides, and then the data points that are located in the same interval will be fully connected.

We give a schematic diagram of the modified frequency-degree mapping algorithm for illustration in the case of integer division in Fig. 10. Here we abbreviate the modified frequency-degree mapping algorithm as MFDM.

As shown in Fig. 10, we select the time series 1, 3, 8, 5, 2, 9, 7, 6 of length 8 with $K = 4$. Firstly, the time series is sorted, and the points on the boundary line, all belong to the smaller intervals below. The data points were divided equally into 4 intervals. First we find the corresponding position of the time series, according to $d = 8/4 = 2$, i.e., $[2 : 2 : 8] = 2, 4, 6, 8$ corresponds to the position of the interval boundaries, so the range of intervals is divided into $(-\infty, 2], (2, 5], (5, 7], (7, 9]$, the time series: $1, 3, 8, 5, 2, 9, 7, 6$ correspond to the intervals as $[1, 2, 4, 2, 1, 4, 3, 3]$. Then the data points are connected to its two nearest neighbors on the left and right and then the data points located in the same interval are fully connected.

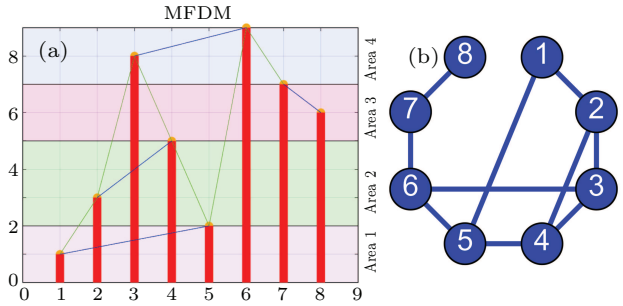


Fig. 10. Panel (a) is sample time series ([1, 3, 8, 5, 2, 9, 7, 6]) and panel (b) is its associated network derived from the modified frequency-degree mapping algorithm.

The case where N does not divide by K: If N does not divide by K, then the data points will be divided into $K+1$ intervals, denoted as $d = N/K$, the time series will be sorted from the smallest to the largest, according to the segmentation of the data points of the time series, and after that, for the data points connected with its left and right nearest neighbors and then the data points located in the same interval will be fully connected. We give a schematic diagram of the modified frequency-degree mapping algorithm in the case of non-integer divisibility in Fig. 11.

As shown in Fig. 11, we select the time series 0.57, 0.22, 0.76, 0.36, 0.7, 0.95, 0.12, 0.82, 0.25, 0.82 with a length of 10, $K = 4$, and firstly, we sort the time series 0.12, 0.22, 0.25, 0.36, 0.57, 0.7, 0.76, 0.82, 0.82, 0.95, according to which the time series data points are then partitioned into intervals according to $[d : d : N]$, i.e., $[2 : 2 : 8] = 2, 4, 6, 8, 10$ positions. Thus, the divided interval range is $(-\infty, 0.22]$, $(0.22, 0.36]$, $(0.36, 0.7]$, $(0.7, 0.82]$, $(0.82, 0.95]$. Therefore, the time series: 0.57, 0.22, 0.76, 0.36, 0.7, 0.95, 0.12, 0.82, 0.25, 0.82 correspond to the intervals [3, 1, 4, 2, 3, 5, 1, 4, 2, 4], and then connects the data points with its two nearest neighbors on the left and right, and then connects the data points located in the same interval.

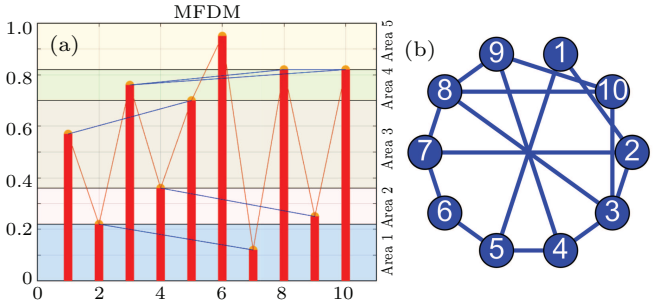


Fig. 11. Panel (a) is a sample time series ([0.57, 0.22, 0.76, 0.36, 0.7, 0.95, 0.12, 0.82, 0.25, 0.82]) and panel (b) is its associated network derived from the modified frequency-degree mapping algorithm.

Remark 2 It can be found that, the original frequency-degree mapping algorithm and modified frequency-degree mapping algorithm are essentially equivalent if the data set to be analyzed is sufficient long (One can eliminate non-divisible segmentation by using data truncation method). But in the case of small data sets, the modified frequency-degree mapping algorithm can definitely preserve more intrinsic information of the original nonlinear time series or complex dynamical system. We can find this advantage in the following part of relevance analysis on original time series and associated networks of this paper.

4. The associated networks family of the unified PWL chaotic system family and their characters

In order to generate the family of associated networks to be analyzed, we firstly generate a time series dataset of the unified PWL chaotic system family. The specific method is as follows. Randomly select initial values within $[0, 1] \times [0, 1] \times [0, 1]$, and traversing the system parameters with a step size of 0.001. Then for each parameter, a time series of length 7001 is generated using the ode45 algorithm with a fixed step size of 0.01. To eliminate transient effects, the first 1001 data points are discarded, leaving a time series of length 6000.

In the numerical study, only the corresponding x-component of the time series is selected, based on the FDM algorithm and MFDM algorithm, the generated time series with a length of 6000 is transformed into a network containing 6000 nodes, and the associated network characteristic quantities are computed. According to Ref. [17], when the length range of a given time series is 1000 to 10000, it may be appropriate to select K being equal to 128 or 256. Therefore, in this paper, the values of $K = 128$ and $K = 256$ are selected for both the FDM and MFDM algorithms. When $K = 128$ and $K = 256$, we first draw the network diagram of the original and modified frequency-degree mapping algorithm for the key parameters at $\alpha = 0.0, 0.125, 1.0$, respectively, as shown in Fig. 12.

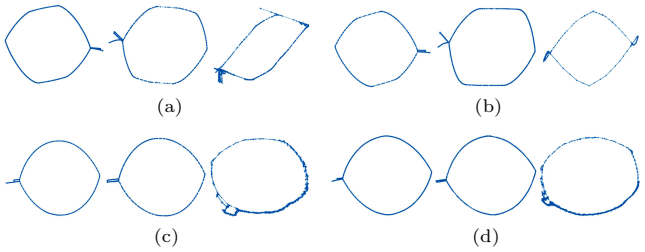


Fig. 12. The associated network derived from the original and modified frequency-degree mapping algorithms. (a) Illustration for the associated networks via original algorithm with parameter $K = 128$, $\alpha = 0.0, 0.125, 1.0$, respectively; (b) illustration for the associated networks via original algorithm with parameter $K = 256$, $\alpha = 0.0, 0.125, 1.0$, respectively; (c) illustration for the associated networks via modified algorithm with parameter $K = 128$, $\alpha = 0.0, 0.125, 1.0$, respectively; (d) illustration for the associated networks via modified algorithm with parameter $K = 256$, $\alpha = 0.0, 0.125, 1.0$, respectively.

When set $K = 128$ and $K = 256$, we transform the generated time series into networks using the modified frequency-degree mapping algorithm and calculate the values of network characteristics as the parameter α varies, as shown in Fig. 13, in both cases, we observed that: after transforming the time series into networks with the modified frequency-degree mapping algorithm, as the parameter α changes from 0 to 1, the average degree, density, global efficiency of the network as a whole show an upward trend. The clustering coefficients of the associated networks initially increase and then decrease. Additionally, the diameter and average path length of the associated networks show an overall decreasing trend.

Then we transform the generated time series into networks using the natural visibility algorithm and horizontal visibility algorithm. We calculate the values of network characteristics as the parameter α varies, as shown in Fig. 14, in both cases, we observed that: as the parameter α changes from 0 to 1, the global efficiency and clustering coefficients of the network show a steady trend. The diameter and average path length of the associated networks initially increase and then decrease. Additionally, the density, average degree of the associated networks show an overall decreasing trend.

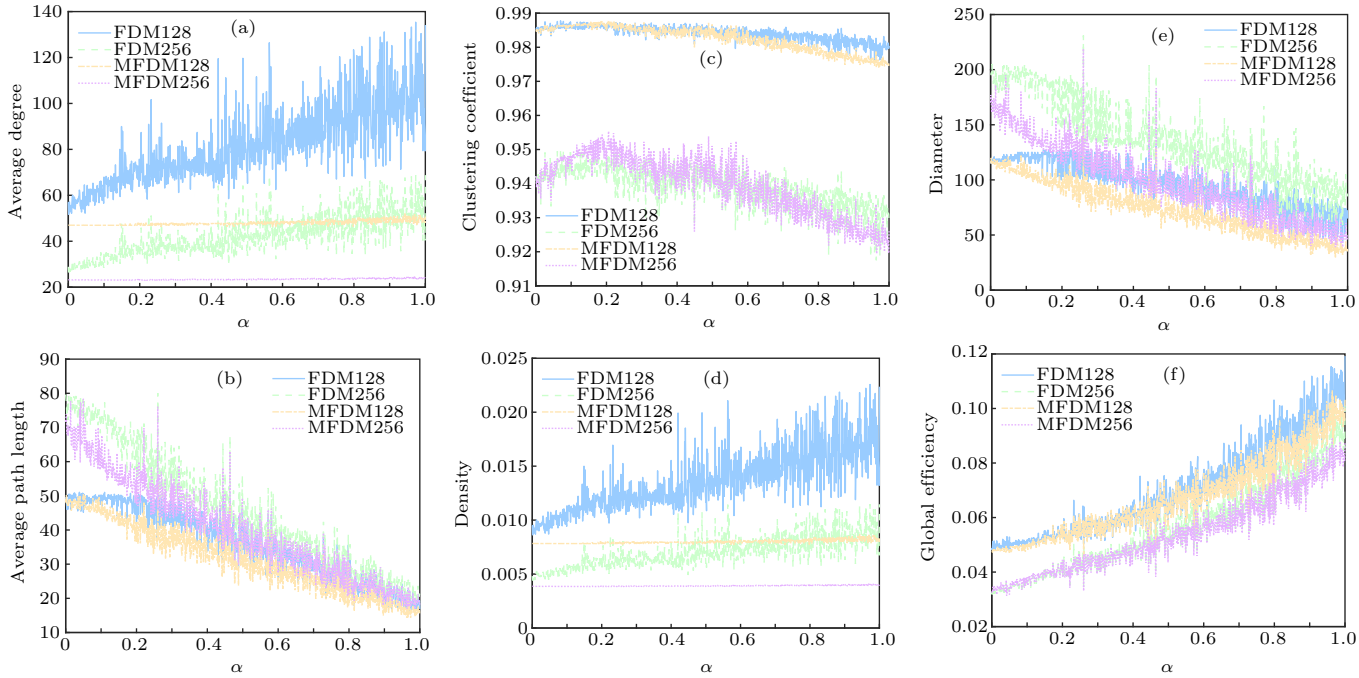


Fig. 13. Schematic diagram of the evolution of digital features of the associated network under the original and modified frequency-degree mapping algorithms with typical parameter conditions when set $K = 128, 256$. (a) Spectrum of variation of average degree, (b) spectrum of variation of average path length, (c) spectrum of variation of clustering coefficient, (d) spectrum of variation of density, (e) spectrum of variation of diameter, (f) spectrum of variation of global efficiency.

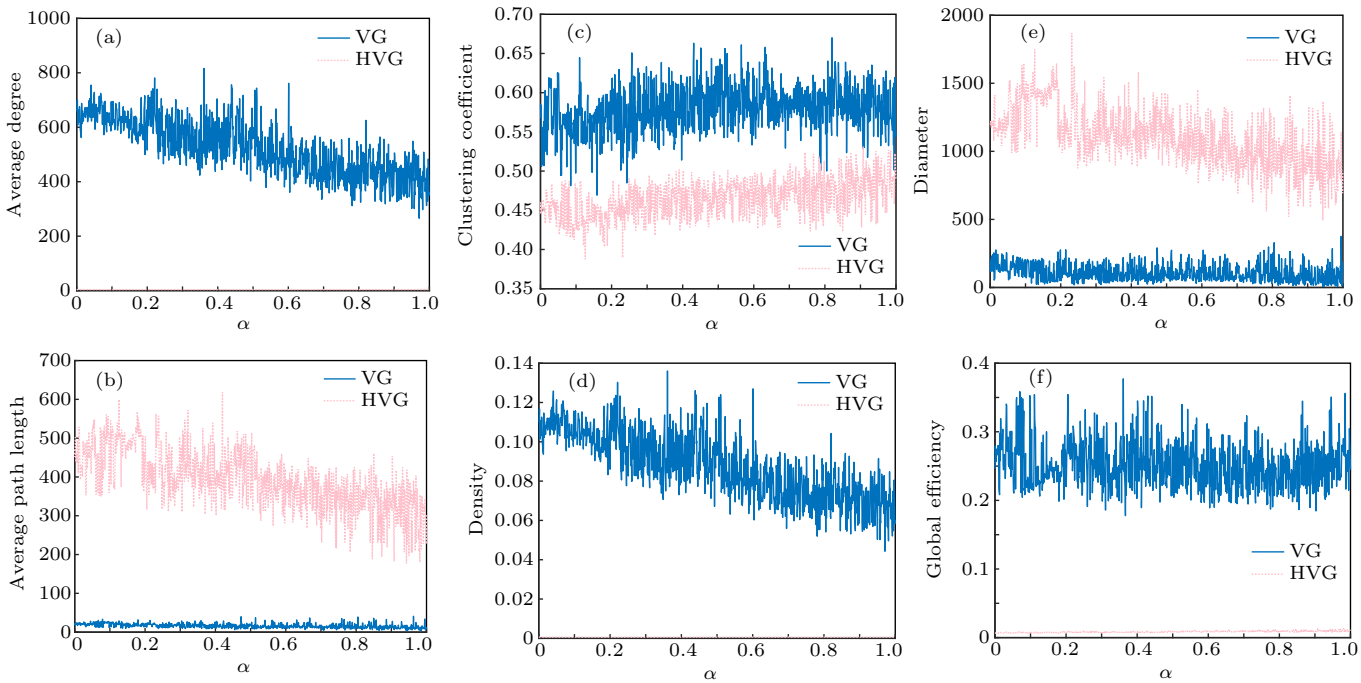


Fig. 14. Schematic diagram of the evolution of digital features of the associated network under the natural visibility algorithm and horizontal visibility algorithm. (a) Spectrum of variation of average degree, (b) spectrum of variation of average path length, (c) spectrum of variation of clustering coefficient, (d) spectrum of variation of density, (e) spectrum of variation of diameter, (f) spectrum of variation of global efficiency.

5. Relevance analysis of unified PWL chaotic system family and its associated network family

In this section, in order to explore the correlation between the network characteristic quantities of the above two algorithms after transforming the time series into networks and the largest Lyapunov exponent under the traditional method, we perform Spearman correlation analysis between them. To facilitate plotting, we use the following notations: network density (density), network diameter (diameter), network average degree (AD), clustering coefficient (C), average path length (APL), global efficiency (GE), largest Lyapunov exponent (LLE).

5.1. The largest Lyapunov exponent versus network fractal dimension

In this section, we calculate the fractal dimension of the network, which is a method to measure the complexity and fractal characteristics of the network structure. By analyzing the fractal dimension of the network, we can understand the internal structure and characteristics of the network more deeply. Based on the box counting method, we calculate the fractal dimension of the associated network generated by the corresponding algorithm.[30]

We calculate the network fractal dimension for the original and modified frequency-degree mapping algorithms when the parameter K is set at $K = 128$ and $K = 256$, as shown in Fig. 15, respectively. We can see that the fractal dimension of the network generally presents an increasing trend with the increase of the key parameter α, i.e., it means the fractal dimension index is increased with key parameter α, which is coincided with the LLE is increased with key parameter α.

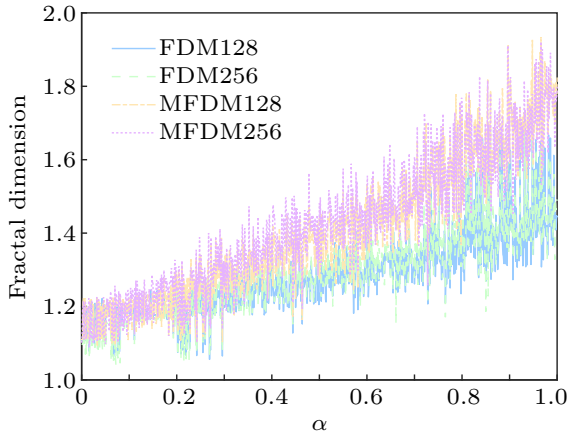


Fig. 15. Schematic diagram of the evolution of digital features of the associated network under the original and modified frequency-degree mapping algorithm and typical parameter conditions when $K = 128$ and when $K = 256$ spectrum of variation of network fractal dimension. We also calculated the spectrum of variation of network fractal dimension via VG and HVG mapping strategies, similar relationships with different scales exist, too. So, it is omitted here.

Then we calculate the Spearman correlation between it and the largest Lyapunov exponent, as shown in Table 1. We find that the quantization level K has little effect on the results, and the correlation of the modified frequency-degree mapping algorithm is higher than that of the original frequency-degree mapping algorithm, indicating that our modified algorithm can reveal the intrinsic characteristics of time series better.

Table 1. The correlation between the largest Lyapunov exponent and network fractal dimension.

Quantization level K	128	256
FDM	0.8561	0.8641
MFDM	0.9143	0.9016

5.2. The largest Lyapunov exponent versus other network characteristics

5.2.1. Under original frequency-degree mapping algorithm when $K = 128$

When the single parameter $K = 128$, we calculated the Spearman correlation coefficient between the network features obtained from the original frequency-degree mapping algorithm and the largest Lyapunov exponent, as illustrated in Fig. 16.

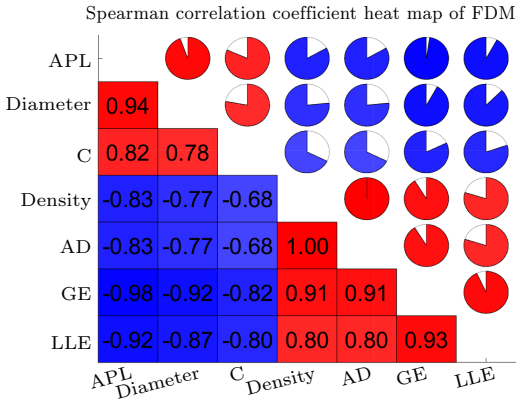


Fig. 16. Heat map of Spearman correlation coefficient under the original frequency-degree mapping algorithm when $K = 128$.

After transforming the time series into networks using the original frequency-degree mapping algorithm, it is found that: the density, average degree, global efficiency of the associated network and the largest Lyapunov exponent of the unified PWL chaotic system family are highly positively correlated, with the correlation coefficients being greater than 0.5, and the correlation coefficients of the strong correlation are 0.8, 0.8, 0.93 respectively. The network diameter, clustering coefficient, and average path length are highly negatively correlated with the largest Lyapunov exponent of the unified PWL chaotic system family, with correlation coefficients of -0.87, -0.80, and -0.92, respectively, suggesting that after the frequency-degree mapping algorithm transforms the time series into networks, the network features of the associated networks can capture the intrinsic properties of the time series just as well as the largest Lyapunov exponent.

5.2.2. Under original frequency-degree mapping algorithm when $K = 256$

When the single parameter K is 256, we calculated the Spearman correlation coefficient between the network characteristics obtained from the original frequency-degree mapping algorithm and the largest Lyapunov exponent, as illustrated in Fig. 17.

After transforming the time series into networks using the original frequency-degree mapping algorithm, it is found that: the density, average degree, global efficiency of the associated network, and the largest Lyapunov exponent of the unified PWL chaotic system family are highly positively correlated, with the correlation coefficients being greater than 0.5,

and the correlation coefficients of the strong correlation are 0.78, 0.78, 0.94, respectively. The network diameter, clustering coefficient, and average path length are highly negatively correlated with the largest Lyapunov exponent of the unified PWL chaotic system family, with correlation coefficients of −0.88, −0.72, and −0.94, respectively, which suggests that after the original frequency-degree mapping algorithm transforms the time series into networks, the network features of the associated networks can capture the intrinsic properties of the time series just as well as the largest Lyapunov exponent.

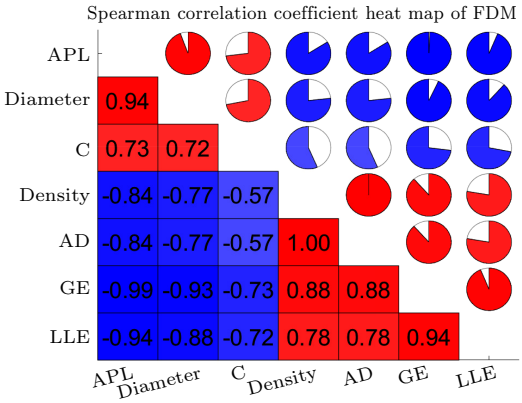


Fig. 17. Heat map of Spearman correlation coefficient under the original frequency-degree mapping algorithm when $K = 256$.

5.2.3. Under modified frequency-degree mapping algorithm when $K = 128$

When the single parameter $K = 128$, we calculated the Spearman correlation coefficient between the network features obtained from the modified frequency-degree mapping algorithm and the largest Lyapunov exponent, as illustrated in Fig. 18.

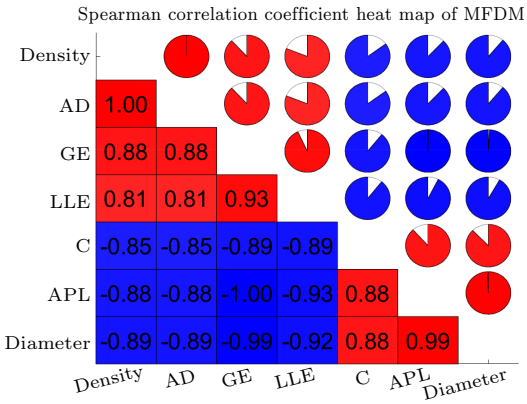


Fig. 18. Heat map of Spearman correlation coefficient under the modified frequency-degree mapping algorithm when $K = 128$.

After transforming the time series into networks using modified frequency-degree mapping algorithm, it is found that: the density, average degree, global efficiency of the associated network are highly positively correlated with the largest Lyapunov exponent of the unified PWL chaotic system family, the correlation coefficients being greater than 0.5. The correlation coefficients of strong correlation are 0.81, 0.81, 0.93, respectively. The network diameter, clustering coefficient, and average path length are highly negatively correlated with the largest Lyapunov exponent of the unified PWL chaotic system family, with correlation coefficients of −0.92, −0.89, and −0.93, respectively, which suggests that after the modified frequency-degree mapping algorithm transforms the time series into networks, the network features of the associated networks can capture the intrinsic properties of the time series just as well as the largest Lyapunov exponent.

5.2.4. Under modified frequency-degree mapping algorithm when $K = 256$

When the single parameter K is 256, we calculated the Spearman correlation coefficient between the network features obtained from the modified frequency-degree mapping algorithm and the largest Lyapunov exponent, as illustrated in Fig. 19.

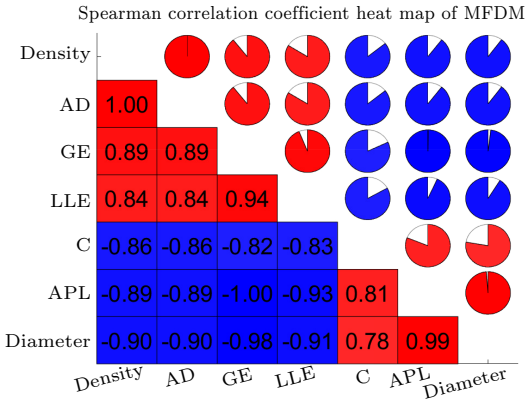


Fig. 19. Heat map of Spearman correlation coefficient under the modified frequency-degree mapping algorithm when $K = 256$.

After transforming the time series into networks using modified frequency-degree mapping algorithm, it is found that: the density, average degree, global efficiency of the associated network, and the largest Lyapunov exponent of the unified PWL chaotic system family are highly positively correlated, with the correlation coefficients being greater than 0.5, and the correlation coefficients of the strong correlation are 0.84, 0.84, 0.94 respectively. The network diameter, clustering coefficient, and average path length are highly negatively correlated with the largest Lyapunov exponent of the unified PWL chaotic system family, with correlation coefficients of −0.91, −0.83, and −0.93, respectively, which suggests that after the frequency-degree mapping algorithm transforms the time series into networks, the network features of the associated networks can capture the intrinsic properties of the time series just as well as the largest Lyapunov exponent.

In order to more conveniently compare the correlation between the network features and the largest Lyapunov exponent under these method mappings, we put the corresponding results in Table 2.

Table 2. The correlation between the largest Lyapunov exponent and network characteristics.

Methods	Density versus LLE	Diameter versus LLE	AD versus LLE	C versus LLE	APL versus LLE	GE versus LLE
FDM ($K = 128$)	0.80	–0.87	0.80	–0.80	–0.92	0.93
MFDM ($K = 128$)	0.81	–0.92	0.81	–0.89	–0.93	0.93
FDM ($K = 256$)	0.78	–0.88	0.78	–0.72	–0.94	0.94
MFDM ($K = 256$)	0.84	–0.91	0.84	–0.83	–0.93	0.94

Remark 3 In order to compare the correlation between the network characteristic quantities and the largest Lyapunov exponent of the network converted by the classical natural visibility algorithm[9] and the horizontal visibility algorithm,[10] the correlation results obtained by the mapping of the two methods are shown in Figs. 20 and 21. We can find that the correlation of these two algorithms is not as high as that of the original frequency-degree mapping algorithm and the modified frequency-degree mapping algorithm.

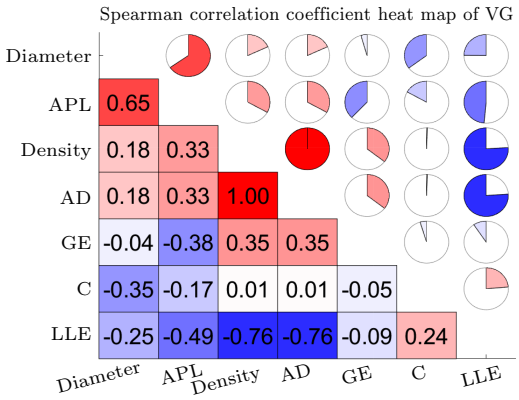


Fig. 20. Heat map of Spearman correlation coefficient under the natural visibility algorithm.

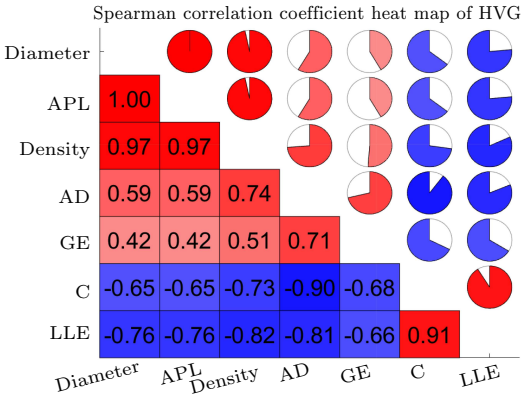


Fig. 21. Heat map of Spearman correlation coefficient under the horizontal visibility algorithm.

In summary, we adopt the original frequency-degree mapping algorithm and consider the positional information of the data points of the time series. Then we propose a modified frequency-degree mapping algorithm. After transforming the time series into networks by these methods, we conduct Spearman correlation analyses between the network characteristics and the largest Lyapunov exponent. We find that in the original and modified frequency-degree mapping algorithms, regardless of whether $K = 128$ or $K = 256$, the network diameter and global efficiency exhibit a strong positive correlation with largest Lyapunov exponent, while network density, average degree, global efficiency display a strong negative correlation with the largest Lyapunov exponent. The correlations obtained by these two algorithms are higher than that obtained by the classical natural visibility algorithm and the horizontal visibility algorithm, indicating that these two algorithms can capture the intrinsic characteristics of time series well. Moreover, the modified frequency-degree mapping algorithm demonstrates higher correlation, indicating that both algorithms effectively capture the evolution patterns of the time series, with the modified algorithm better revealing the intrinsic characteristics of the time series.

6. Discussion and conclusion

In this paper, numerical analysis on the unified PWL chaotic family and its associated networks are carried out from a network analysis perspective, which focused on the possibility for dynamics analysis of the unified PWL chaotic family via network analysis on the associated networks of related dynamical systems. Specifically, in this paper, we computed the associated network families' characteristics by using both the original and modified frequency-degree mapping algorithms, with quantization levels of 128 and 256, respectively. After transforming the time series into networks, we conducted Spearman correlation analyses between these network characteristics and the largest Lyapunov exponent.

Our findings revealed that, by using the aforementioned algorithms, network density, average degree, network global efficiency, and network fractal dimension exhibit a strong positive correlation with the largest Lyapunov exponent. Conversely, the network diameter, network clustering coefficient, and average path length are highly negatively correlated with the largest Lyapunov exponent. Therefore, frequency-degree mapping strategy can effectively analyze and understand the dynamic behavior of the system after mapping the time series into a network. The generated network features can effectively capture the changes in the dynamic behavior of the system. The high correlation between the network characteristic quantities and the largest Lyapunov exponent enhances the effectiveness of our proposed mapping method, indicating that important information about the system behavior can be obtained through network features. It should be addressed that, the modified frequency-degree mapping algorithm demonstrates

higher correlation, which indicated that both frequency-degree mapping algorithms can effectively capture the evolution patterns of the nonlinear time series, i.e., the modified frequency-degree algorithm can reveal the intrinsic characteristics of the related nonlinear time series better than the original frequency-degree mapping algorithm, the VG, and HVG mapping algorithm.

In conclusion, the numerical study in this paper shows that there is some kind of intrinsic consistency between the amount of network features and the variation of the largest Lyapunov exponent. The network characteristic quantities can also characterize the nonlinear properties of the system. The frequency-degree mapping strategy is effective in characterizing the intrinsic dynamics of the system. In the future, we will continue to discuss the potential value of other time series transformation algorithms in nonlinear dynamic analysis.

References

[1] Zou Y, Donner R V, Marwan N, Donges J F and Kurths J 2019 *Phys. Rep.* **787** 1

[2] Silva V F, Silva M E, Ribeiro P and Silva F 2021 *WIREs Data Min. Knowl. Discov.* **11** e1404

[3] Wolf A, Swift J B, Swinney H L and Vastano J A 1985 *Physica D* **16** 285

[4] Grassberger P and Procaccia I 1983 *Phys. Rev. Lett.* **50** 346

[5] Grassberger P and Procaccia I 1983 *Phys. Rev. A* **28** 2591

[6] Zhang J and Small M 2006 *Phys. Rev. Lett.* **96** 238701

[7] Bradley E and Kantz H 2015 *Chaos* **25** 097610

[8] Azizi Hadis and Sulaimany S 2024 *IEEE Access* **12** 93517

[9] Lacasa L, Luque B, Ballesteros F, Luque J and Nuno J C 2008 *Proc. Natl. Acad. Sci. USA* **105** 4972

[10] Luque B, Lacasa L, Ballesteros F and Luque J 2009 *Phys. Rev. E* **80** 046103

[11] Marwan N, Donges J F, Zou Y, Donner R V and Kurths J 2009 *Phys. Lett. A* **373** 4246

[12] Campanharo A S, Sirer M I, Malmgren R D, Ramos F M and Amaral L A N 2011 *PloS ONE* **6** e23378

[13] Zhou T T, Jin N D, Gao Z K and Luo Y B 2012 *Acta Phys. Sin.* **61** 030506 (in Chinese)

[14] Lacasa, L, Nicosia V and Latora V 2015 *Sci. Rep.* **5** 15508

[15] Wen T, Chen H and Cheong K H 2022 *Nonlinear Dyn.* **110** 2979

[16] Donner R V, Small M, Donges J F, *et al*. 2011 *Int. J. Bifurc. Chaos* **21** 1019

[17] Li X, Yang D, Liu X and Wu X M 2012 *IEEE Circ. Syst. Mag.* **12** 33

[18] Sun X, Small M, Zhao Y and Xue X 2014 *Chaos* **24** 024402

[19] Gao Z K, Hu L D and Jin N D 2013 *Chin. Phys. B* **22** 050507

[20] Walker D M, Correa D C and Small M 2018 *Chaos* **28** 013101

[21] Liu J, Wang H, Xu H, Bao S and Li L 2020 *Chinese Control and Decision Conference*, August 22–24, 2020, Hefei, China, p. 4868

[22] Wang X, Han X, Chen Z, Bi Q, Guan S and Zou Y 2022 *Chaos, Solitons and Fractals* **159** 112026

[23] Wang S, Li P, Chen G and Bao C 2024 *Chaos* **34** 043145

[24] Lü J H, Chen G R and Chen D Z 1993 *Int. J. Bifurcat. Chaos* **14** 1507-1537

[25] Liu J, Lu J and Wu X 2004 *ICARCV 8th Control, Automation, Robotics and Vision Conference,* December 6–9, 2004, Kunming, China, p. 1368

[26] Baghious E H and Jarry P 1993 *Int. J. Bifurcat. Chaos* **3** 201

[27] Ozoguz S, Elwakil A S and Kennedy M P 2002 *Int. J. Bifurcat. Chaos* **12** 1627

[28] Aziz-Alaoui M and Chen G 2002 *Int. J. Bifurcat. Chaos* **12** 147

[29] Nabil H and Tayeb H 2024 *Chin. Phys. B* **33** 120503

[30] Zhao P C, Wei H J, Xu Z K, Chen D Y, Xu B B and Wang Y M 2023 *Chin. Phys. B* **32** 090503

[31] Liu T and Xia X 2024 *Chin. Phys. L* **41** 017102

[32] Song C M, Gallos L K, Havlin S and Makse H A 2007 *J. Stat. Mech.-Theory. E* **2007** P03006